Solvent Effects on the Fluorescence Quenching of Tryptophan by Amides via Electron Transfer. Experimental and Computational Studies†

Pedro L. Muiño*,‡ and Patrik R. Callis§

Department of Chemistry, Saint Francis University, Loretto, Pennsylvania 15940, and Department of Chemistry and Biochemistry, Montana State University, Bozeman, Montana 59717

Received: December 6, 2007; Revised Manuscript Received: March 13, 2008

Hybrid quantum mechanical/molecular mechanics (QM-MM) calculations [Callis and Liu, *J. Phys. Chem. B* **2004**, *108*, 4248−4259] make a strong case that the large variation in tryptophan (Trp) fluorescence yields in proteins is explained by ring-to-backbone amide electron transfer, as predicted decades ago. Quenching occurs in systems when the charge transfer (CT) state is brought below the fluorescing state (^1L_a) as a result of strong local electric fields. To further test this hypothesis, we have measured the fluorescence quantum yield in solvents of different polarity for the following systems: *N*-acetyl-L-tryptophanamide (NATA), an analogue for Trp in a protein; *N*-acetyl-L-tryptophan ethyl ester (NATE), wherein the Trp amide is replaced by an ester group, lowering the CT state energy; and 3-methylindole (3MI), a control wherein this quenching mechanism cannot take place. Experimental yields in water are 0.31, 0.13, and 0.057 for 3MI, NATA, and NATE, respectively, whereas, in the nonpolar aprotic solvent dioxane, all three have quantum yields near 0.35, indicating the absence of electron transfer. In alkyl alcohols the quantum yield for NATA and NATE is between that found for water and that found for dioxane, and it is surprisingly independent of chain length (varying from methanol to decanol), revealing that microscopic H-bonding, and not the bulk dielectric constant, dictates the electron transfer rate. QM-MM calculations indicate that, when averaged over the six rotamers, the greatly increased quenching found in water relative to dioxane can be attributed mainly to the larger fluctuations of the energy gap in water. These experiments and calculations are in complete accord with quenching by a solvent stabilized charge transfer from ring to amide state in proteins.

Introduction

The sensitivity of tryptophan (Trp) fluorescence intensity to protein/solvent environment is used extensively to monitor a variety of protein transformations.[1,2] Quantitatively, the fluorescence quantum yield (Φ_f) of Trp in proteins varies from near 0.35 down to 0.01 or less.[1] For nearly 40 years, this stood as a puzzle because Φ_f for the light-absorbing part of Trp, well represented by 3-methylindole (3MI), is virtually independent of solvent polarity, being always near 0.35.[3] Until recently, it was not possible to predict, even qualitatively, the relative intensities from structural information.

Inspired by incisive experiments[4−6] strongly supporting the long-standing hypothesis that efficient quenching can be caused by electron transfer (ET) from the excited indole ring to a nearby amide,[5−8] we have recently demonstrated reasonable success at predicting the fluorescence yields and average lifetimes for 20 single-Trp proteins.[9,10] The method has since been useful for understanding Trp fluorescence in a number of proteins.[11−13] The method uses hybrid quantum mechanics/molecular mechanics (QM/MM) to compute the relative energies of the fluorescing (^1L_a) and the charge transfer (CT) states during 60−300 ps molecular dynamics (MD) simulations. The relative electrostatic potential of the ring and amide atoms is computed from protein and solvent partial charges, and fed into the quantum mechanical part. The lowest energy CT state is invariably found to be well described by transfer of an electron from the indole ring to the lowest unoccupied π^* molecular orbital (MO) localized on the nearest backbone amide.[10] The observed quantum yields were found to correlate well with the computed energy gap between the CT and ^1L_a state while assuming a constant electronic coupling. Recent *ab initio* computations of the electronic coupling as a function of rotamer conformation indicate no correlation of the quantum yield with average coupling strength.[14]

While the predictive success of the method provides circumstantial evidence for this mechanism, no direct evidence for the CT state currently exists. One important check, however, would be to determine whether the quenching is eliminated in nonpolar solvents, wherein the reorganization energy to stabilize a CT state would be severely reduced. The activation energy would be increased, and little or no ET-based quenching would be expected. (A particularly unequivocal example is provided by Wasielewski et al.[15]) In this paper, we report a systematic study of the effect of solvent polarity on the fluorescence quantum yield of *N*-acetyl-L-tryptophanamide (NATA), an analogue for Trp in a protein, *N*-acetyl-L-tryptophan ethyl ester (NATE), wherein the C-terminal amide is replaced by an ester group, lowering the CT state energy; and 3MI, a control where this quenching mechanism cannot take place. See Figure 1 for the structure of NATA. Three classes of solvent are investigated: water, *n*-alkyl alcohols, and ethers. In water, the quantum yield of NATA has long been known to be reduced from that of 3MI by 50%.[7] In the ethers, dioxane, and tetrahydrofuran (THF),

† Part of the "J. Michael Schurr Special Section".

* Corresponding author. Phone: 1 (814) 472-3084. Fax: 1 (814) 472-2773. E-mail: pmuino@francis.edu.
‡ Saint Francis University.
§ Montana State University.

10.1021/jp711513b CCC: $40.75
Published on Web 08/02/2008

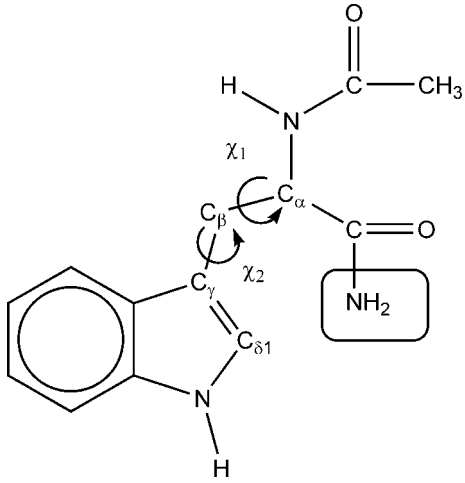

Figure 1. Molecule of NATA with the torsional angles that identify the different conformers. The hydrogens attached to the carbon atoms are not explicitly written. NATE, which is structurally similar, differs from NATA in the replacement of an ethoxy group ($-O-CH_2CH_3$) for the amino group ($-NH_2$) located in the box.

the solvent cannot donate an H-bond and is expected to be less stabilizing for the CT state. In the longer chain alcohols, the dielectric constant is low, but there is capability for both donation and acceptance of an H-bond. Experimental results are found to be generally consistent with ET to the amide.

QM/MM simulations of the Φ_f values for NATA and NATE in dioxane, octanol, and water are also presented.

Methods

Materials. NATA (98%, 856754, batch # 18725PA), NATE (85772-6, lot # 20022PN), and 3MI (lot # 11822CF), were obtained from Sigma-Aldrich and used without further purification. Water was deionized ($R > 18$ MΩ). Methanol was acquired from Science Kit and Boreal Laboratories (100%, 83745, lot # AD-5178). Decane and THF were obtained from Fisher Scientific: decane, 99.2%, 02128, lot # 963655; THF, 99.9%, 020587, lot # 911321. All other solvents were purchased from Sigma-Aldrich: 1-butanol (anhydrous, 99.8%, 281549, batch # 09446HA), 1-pentanol (99+%, 138975, batch # 01959AB), 1-hexanol (anhydrous, 99+%, 471402, batch # 03143BB), 1-heptanol (~99%, H-6129, lot # 111K3685), 1-octanol (anhydrous, 99+%, 297887, batch # 04542DO), 1-decanol (99+%, 239763, batch # 10509DQ), methylcyclohexane (anhydrous, ≥99+%, 300306, lot # TA 01738PA), and 1,4-dioxane (for UV spectroscopy, ≥99.8%, 42500, lot and filling codes 44480/1 44602994).

Experiment. *Infrasil* cuvettes were purchased from Starna. The nominal usable range specified by the manufacturer was from 220 to 3800 nm. Solutions were prepared fresh before each experiment. Concentrations were in the range of 5 to 50 μM, (with absorbances between 0.025 and 0.25 at 280 nm). The samples were then placed in a thermostatted bath at 20 °C and degassed before fluorescence was collected. Degassing was accomplished by bubbling nitrogen for 10 min (if the solvent was water or an alcohol), or 20 min (for nonpolar solvents) in order to eliminate dissolved oxygen. Increasing the bubbling times had no effect.

Absorbances for each sample were collected using a Perkin-Elmer Lambda 2S UV−vis spectrophotometer. An identical cuvette filled with solvent was always used as a zero. Spectra were collected from 350 to 260 nm. The value measured at 280 nm was subsequently used in the calculation of the quantum yield (see eq 1).

Fluorescence measurements were performed in a Fluoromax 3 fluorometer with a cooled PMT and photon counting capability. The spectra were collected from 285 to 500 nm (λ_{exc} = 280.0 nm; step: 0.5 nm; integration time: 0.50 s; slits for both excitation and emission monochromator: 0.50 mm, which represents a resolution of 1.6 nm). Spectra of the pure solvents were collected and subtracted from the spectrum of each sample in order to eliminate any potential luminescence from a contaminant. The cuvette holder was adjusted with a micrometer in order to position the fluorescing volume just inside the inside edge of the first cuvette wall, thereby avoiding concentration effects. With this procedure, we have measured quantum yields using solutions with absorbances from 0.1 to 0.5, at 280 nm, with no significant differences. From the collected data, the quantum yield is calculated using eq 1.

$$\Phi_{system} = \Phi_{ref} \frac{\text{Fluorescence (system)}}{\text{Fluorescence (ref)}} \frac{A_{ref}}{A_{system}} \qquad (1)$$

As a reference, we have used the system 3MI−water, for which available literature values range from 0.29 at 20 °C,[3] 0.34 at 20 °C,[16] and 0.34 at 25 °C.[17] We settled on an average of the two measurements, at 20 °C, of 0.31 as the reference quantum yield. This fits well with corresponding values of $k_r = 4 \times 10^7$ s^{-1} and $k_{nr} = 9 \times 10^7$ s^{-1} for which a value of the quantum yield can be obtained: $\Phi_f = k_r \times (k_r + k_{nr} + k_{et})^{-1} = 0.31$ in the absence of ET. These values will be used in the computation of quantum yields (see Theory section). A_{ref} and A_{system} (in eq 1) are the absorbances of the reference solution (3MI−water) and of the sample, respectively, at 280 nm and 20 °C. The fluorescence intensities used to calculate the quantum yields (with eq 1) were obtained by integration of the full fluorescence trace. The spectra were not corrected for the detector response. A minimum of six experiments (except four experiments for NATA−THF and NATE−octanol) were performed for each sample and averaged.

Computation. A hybrid molecular dynamics/semiempirical molecular orbital method was used to calculate transition energies between the ground-state and two excited states, ^1L_a (S_1) and a higher energy CT state, as a result of solvent motion. The method has been described in detail before.[10] Briefly, the molecular dynamics program CHARMM is used to model the motion of a system containing a central chromophore molecule (NATA or NATE) surrounded by a drop (20 Å radius) of solvent at 300 K. The number of solvent molecules is chosen to match literature values of the density at 25 °C. Every 10 steps, (i.e., 10 fs), the coordinates of the system are extracted and used as input for a semiempirical molecular orbital program, Zerner's INDO/S-CIS[18] ("Zindo"), which treats the chromophore explicitly. The solvent molecular orbitals are not included in the calculation, but the solvent effect on the chromophore energy levels is modeled by inclusion of the collective electrostatic perturbation on the Fock matrix. INDO/S-CIS provides information on the transition energies between the desired states, as well as information on the partial charges on the atoms that make up the chromophore. These charges are fed back into the dynamics simulation to provide an updated field that interacts with the solvent. Six different conformations of NATA and NATE were used (see Figure 1 to identify the torsions). The label *m*(inus) indicates a negative angle (−60°or χ_1 and −90° for χ_2). The label *p*(lus) indicates a positive angle (+60° for χ_1 and +90° for χ_2). The label *t*(rans) indicates a dihedral angle of 180°. Thus, the *mm* conformer indicates $\chi_1 = -60°$ and $\chi_2 =$

−90°. Other conformers are: *mp* (−60°, +90°), *pm* (+60°, −90°), *pp* (+60°, +90°), *tm* (180°, −90°), and *tp* (180°, +90°). Calculations were performed with simulation times of 60 ps. In several cases, we extended these calculations for an additional 250 ps interval. The calculated quantum yields for the longer simulations were quite similar to those from the 60 ps simulations.

The charges on the atoms of the chromophore were those calculated by INDO/S for the ^1L_a state. In order to examine the behavior of the CT state more effectively, the bond lengths in the indole ring were kept fixed throughout the simulation, at values corresponding to the CT state minimum. At the end of the 60 ps simulations, the chromophore charges were switched from ^1L_a state values to CT state values. The subsequent evolution of the system for 30 additional picoseconds provides an indication of the reorganization time and energy.

Theory. The Fermi Golden Rule for the ET rate constant (k_{et}) is given by[19−21]

$$k_{et} = 2\pi\hbar^{-1}\langle V^2\rangle\rho(\Delta E_{00}) \quad (2)$$

where V is the electronic matrix element coupling the CT and ^1L_a states, and $\rho(\Delta E_{00})$ is the density of final states associated with a difference in zero point energy, ΔE_{00}, which is[20,22]

$$\rho(\Delta E_{00}) = \int F_{D\rightarrow D^+}(\Delta E_{00},E)F_{A\rightarrow A^-}(\Delta E_{00},E)\mathrm{d}E \quad (3)$$

This is the overlap of the photoelectron spectrum on the indole ring (the electron donor) with that of the acceptor anion. It is assumed that fluctuations in the environment modulate ΔE_{00} randomly and rapidly on the fluorescence lifetime scale, leading to a Gaussian distribution for ΔE_{00}. This leads to the following expression for the ET rate constant:

$$\langle k_{et}\rangle = 4\pi^2 c\langle|V^2|\rangle(2\pi\sigma^2)^{-\frac{1}{2}}\int \rho_{FC}(\Delta E_{00}) \times \exp\left[-\frac{1}{2}\left(\frac{\Delta E_{00}-\overline{\Delta E_{00}}}{\sigma}\right)^2\right]\mathrm{d}\Delta E_{00} \quad (4)$$

where all energy units are in cm^{-1}, $c = 3 \times 10^{10}$ cm s^{-1}, and σ is the Gaussian width (standard deviation) of the ΔE_{00} distribution. In this expression, the Gaussian is the function φ_{AB}, the probability density for finding a potential energy difference ΔE_{00} during the MD trajectory, featured by Tachiya[21] in his generalization of Marcus theory.[19]

We use $V = 10.0$ cm^{-1} for all conformations of NATA and NATE and $\Delta E_{00} = \Delta E_{vert} - 4000$ cm^{-1}. These values produced an acceptable correlation between computed and experimental quantum yields for Trp in proteins.[10]

Quantum yield variation was assumed to be entirely determined by variations in the ET rate constant, k_{et}, by assuming the ^1L_a radiative rate constant and nonradiative rate constant, k_r and k_{nr}, were constant with values given above.

Results

Figure 2 shows fluorescence spectra of NATA (normalized by dividing by the absorbance of each sample) in three solvents representative of the three solvent classes: dioxane (low polarity and aprotic), 1-octanol (medium polarity and protic), and water. The observed quantum yield decrease (from low to high polarity) is consistent with the predictions of ET-based fluorescence quenching.[15,21]

The quantum yields for all the systems studied are summarized in Table 1. Agreement with previously published values when available is satisfactory, except for the hydrocarbons. For

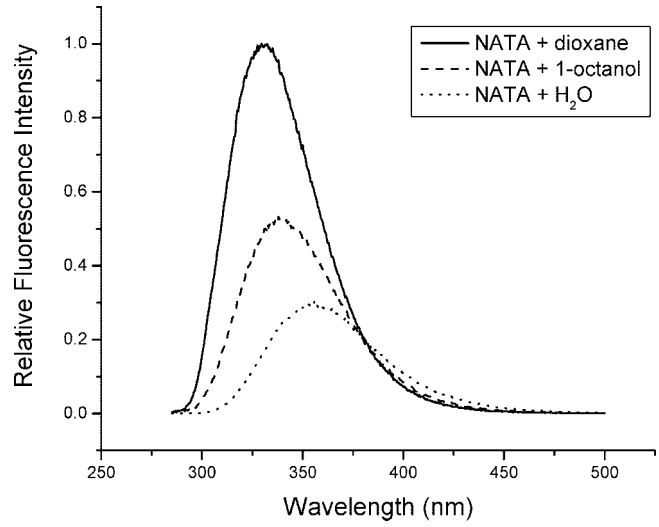

Figure 2. Fluorescence spectra for NATA in dioxane (solid line), 1-octanol (dashed line), and H_2O (dotted line). The spectra have been normalized by dividing by the absorbance of the sample (at 280 nm). The scale of the *y*-axis is arbitrary, and the traces have been multiplied by a factor (same for all three) so that the maximum value of the fluorescence for the NATA+dioxane trace is set at 1.0. Each trace represents an average of (at least) six experiments.

3MI, Meech et al.[3] report 0.40 in cyclohexane, 0.38 in THF, and 0.35 in butanol. Our values for the hydrocarbons ranged from 0.22 to 0.27. However, for the more relevant solvents, dioxane and THF (which dissolve NATA and NATE), agreement is much better. For NATA in water we find 0.13 compared to 0.14[16] and for NATE in water, we find 0.06 compared to 0.066[16] and 0.06.[6]

The last two columns of the Table 1 compare the ratio of the quantum yields for NATA or NATE (for which intramolecular ET is possible) to the quantum yields for 3MI (for which intramolecular ET is not possible). The general result is that Φ_f is very high for 3MI in all solvents. For NATA in dioxane and THF, Φ_f is similarly high. A striking and revealing finding is that Φ_f is *always* ∼0.20 for NATA for the entire range of alcohols, although the dielectric constant varies from 8.3 to 33 from decanol to methanol. For NATE, which has the better electron acceptor group, a similar pattern is observed, except that Φ_f is ∼0.10 for all the alcohols. For both NATA and NATE in water there is a substantial drop to 0.13 and 0.06, respectively. These results are quite consistent with the prediction that low solvent polarity will result in higher quantum yields relative to water for NATA and NATE.

Predicted quantum yields from QM/MM computations for six different rotational conformers of NATA and NATE in three representative solvents (water, 1-octanol, and dioxane) are shown in Table 2. (Information on the torsional angles can be seen in Figure 1.) The quantum yields are calculated (see Methods and Theory sections) by assuming the ET is responsible for the quenching. Large differences in average ET rate were found for different rotamers, but when averaged over the six rotamers, the computed values are in reasonable agreement with experiment for NATA. The Zindo method does not seem to distinguish well between the amide and the ethyl ester as an electron acceptor.

Figure 3 shows representative trajectories for NATA in the three solvents used for Table 2. The conformers chosen (*mp* in dioxane, *mm* in 1-octanol and water) are the ones whose calculated Φ_f best match the average for all conformers in a given solvent. During the first 60 ps of the simulations, the

TABLE 1: Experimental Quantum Yields for NATA, NATE, and 3MI in Different Solvents

solvent	NATA	NATE	3MI	Φ_{NATA}/Φ_{3MI}	Φ_{NATE}/Φ_{3MI}
decane			0.27 ± 0.01		
methylcyclohexane			0.22 ± 0.01		
cyclohexane			0.24 ± 0.02		
dioxane	0.36 ± 0.02	0.31 ± 0.01	0.37 ± 0.02	0.98	0.83
THF	0.31 ± 0.02		0.32 ± 0.02	0.96	
decanol	0.19 ± 0.01		0.36 ± 0.02	0.53	
octanol	0.21 ± 0.01	0.11 ± 0.01	0.36 ± 0.01	0.59	0.29
heptanol	0.20 ± 0.01		0.37 ± 0.01	0.53	
hexanol	0.20 ± 0.02	0.10 ± 0.01	0.36 ± 0.01	0.54	0.28
pentanol	0.20 ± 0.01		0.37 ± 0.01	0.54	
butanol	0.19 ± 0.02	0.11 ± 0.01	0.37 ± 0.01	0.52	0.28
methanol	0.18 ± 0.01	0.089 ± 0.002	0.33 ± 0.02	0.53	0.27
water	0.13 ± 0.01	0.057 ± 0.001	0.31 ± 0.01	0.40	0.18

TABLE 2: Calculated Quantum Yields for NATA and NATE[a]

	NATA			NATE		
rotamer (χ_1,χ_2)	water	octanol	dioxane	water	octanol	dioxane
mm: (−60°, −90°)	0.091	0.24	0.26	0.29	0.30	0.31
mp: (−60°, +90°)	0.20	0.30	0.27	0.30	0.31	0.31
pm: (+60°, −90°)	0.071	0.12	0.23	0.080	0.18	0.27
pp: (+60°, +90°)	0.17	0.26	0.29	0.18	0.20	0.30
tm: (−180°, −90°)	0.062	0.048	0.29	0.20	0.14	0.29
tp: (+180°, +90°)	0.062	0.29	0.30	0.11	0.089	0.31
Average	**0.11**	**0.21**	**0.27**	**0.19**	**0.20**	**0.30**
Experimental[b]	**0.13**	**0.21**	**0.36**	**0.057**	**0.11**	**0.31**

[a] $V = 10$, $D = -4000$ cm^{-1}. The highest possible calculated yield with our current parameters is 0.31; see Theory section. [b] This work.

chromophore electron density is that of the ^1L_a state. After 60 ps, the charges are instantaneously switched to match those of the CT state. In the suddenly produced charge-separated state, solvent molecules quickly relax to stabilize the new electron density. Figures similar to Figure 3, corresponding to all 36 trajectories evaluated (two chromophores, NATA and NATE, in six conformations for three different solvents) are available as Supporting Information.

An interesting—and perhaps surprising—aspect of the results is the relative insensitivity of the CT−^1L_a energy gap to solvent polarity. This can be seen in Figure 3 and in the Supporting Information. In water, the ^1L_a transition energy is ∼2000 cm^{-1} lower than in the nonpolar solvents, in agreement with considerably red-shifted fluorescence from NATA in water relative to nonpolar solvents.[16] A similar lowering of the CT state in water is found in the simulations.

Figure 4 shows that, when averaged over all rotamers, there is little difference in the energy gap for dioxane and water while in the ^1L_a state. But we observe 50% larger fluctuations in the gap relative to those in dioxane, which facilitates ET. This is emphasized by the large relaxation after the charges are switched to those of the CT state. Thus, if solvent fluctuations ever cause an inversion of states that leads to ET, this inversion would usually be permanent. In octanol and dioxane, the fluctuations, although smaller than in water, are surprisingly large (∼12000 cm^{-1} = 1.5 eV). Furthermore, the similar energies of the CT and ^1L_a states following in the relaxed CT state indicate that should this transfer take place, it may not be permanent. For dioxane, the CT state has the smallest energy drop following ET. This picture is consistent with a low quenching scenario (high quantum yield), observed experimentally.

We have analyzed some of the conformations with the smallest gaps between the states, (less than 1000 cm^{-1}). By calculating the contribution of each solvent molecule to the lowering of the energy of the CT state, we can make the following observations. For NATA + water, 10−12 molecules significantly contribute to the stabilization. It is common, however, to find that 1−2 molecules contribute more than half the total. These two molecules are typically both making an H-bond with the carbonyl of the electron-accepting amide. It is typical during such fluctuations to find more water oxygen atoms than hydrogens near the indole ring. During rare extreme fluctuations that stabilize the CT state by as much as 2.5 eV below the mean, as many as four such H-bonds have formed.

For NATA in octanol, the majority of the energy stabilization results from the effect of 4−6 solvent molecules located closest to the chromophore. These molecules are mainly concentrated near the amide portion of the NATA molecule, but the bulkiness of the hydrocarbon chain permits typically only one H-bond (occasionally two) with the amide carbonyl. Low-energy conformations also usually have the O of one or two octanols near the indole ring. The solvent appears to form a micelle-like structure, with the polar part surrounding the amides.

For NATA in dioxane, the CT state is found to be stabilized by fluctuations that place several O atoms near the indole ring and no O atoms near the amide carbonyl bond.

Discussion

The aim of these experiments was to test the hypothesis that no significant quenching would be observed for NATA (and perhaps NATE) in nonpolar solvents such as dioxane, a reasonable expectation if the quenching is due to intramolecular ET. Indeed, the results do indicate little or no ET for NATA and NATE in dioxane.

Our computational procedure is based explicitly upon the probability density for electric potential difference for an electron on the acceptor relative to the donor, φ_{AB}, introduced by Tachiya[21] in a generalization of Marcus theory. Tachiya has noted that use of φ_{AB} is entirely equivalent to the generation of a free energy parabola for each state. In this view, the solvent dependence of the average vertical energy gap is due entirely to the difference in *electronic* polarization, which is essentially negligible. Most of the solvent dependence resides in the reorganization energy (λ).[19,21] λ is expected to increase with the static dielectric constant (dominated by the reorientational component), i.e., with increasing polarity. Along with increased λ comes larger amplitude of fluctuation,[21,23] which leads to increased ET rate, and faster, higher amplitude relaxation to a permanently dark state (quenching). The energy gap, amplitude of the fluctuations, and relaxation amplitudes seen in Figure 3 (as well as those in the Supporting Information) are all consistent with this picture.

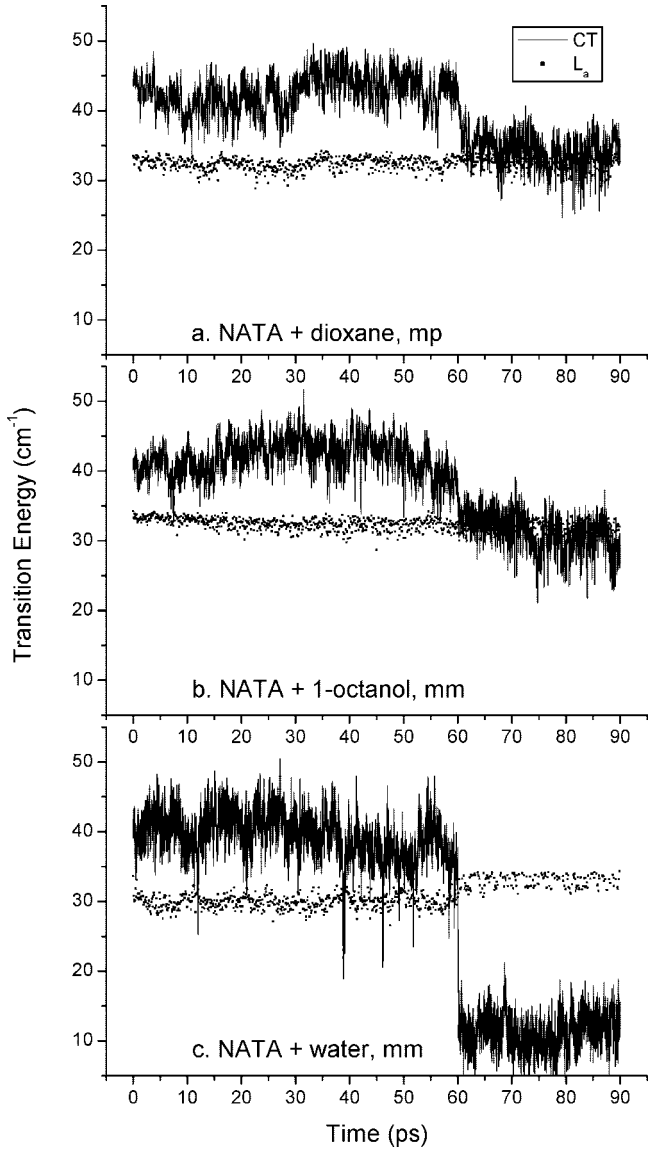

Figure 3. INDO/S-CIS values for the transition energies of the CT and ^1L_a states (CT - S_0, and ^1L_a - S_0) for NATA in (a) dioxane, (b) 1-octanol, and (c) H_2O. The trajectories correspond to the *mp* conformer in dioxane and the *mm* conformers in 1-octanol and water (see Figure 1 and Table 2 for details). These conformations have calculated quantum yields that best match the calculated average values for each solvent. The chromophore is in the ^1L_a state for the first 60 ps of each trajectory and in the CT state for the last 30 ps.

One of the most interesting results emerging from this study is the near independence of Φ_f for the family of alcohols, whose bulk dielectric constants range from 8.3 for decanol to 33 for methanol. This is consistent with an interpretation that the CT state is stabilized primarily through local hydrogen bonding by one or two alcohol hydroxyls, as opposed to a reaction field that is proportional to the static dielectric constant, and that hydroxyl access is similar for all straight chain alcohols. Inspection of models supports this interpretation.

The fluorescence decay of NATA in water is well-known to be described by a single exponential (decay constant = 3 ns).[6,16] This contrasts with the observation that Trp fluorescence in proteins and other small peptides often show nonexponential decay.[1,2] Petrich et al.[6] have made a compelling case that NATA rotamers do not rapidly interconvert during the excited-state lifetime, but rather that each rotamer has the same lifetime because, in each rotamer, the indole ring is, on average,

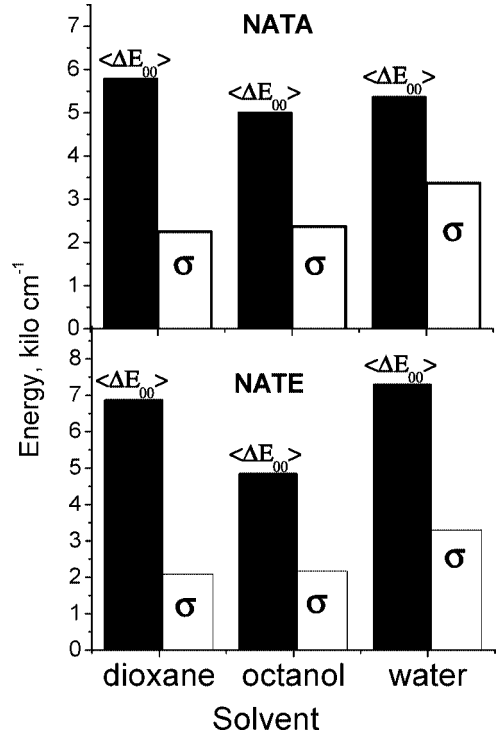

Figure 4. Average computed zero-point CT−^1L_a energy gap, ΔE_{00}, and standard deviation, σ, averaged over the 60 ps simulations for the six rotamers for NATA and NATE in dioxane, octanol, and water.

equidistant from two amide carbonyl carbons. The simulation results shown in Table 2 indicate that substantially different lifetimes would be found for the different rotamers. We believe that longer simulations are likely to produce more similar lifetimes, but that is left for future work.

One may argue that, while our results are consistent with quenching from a CT state, the nature of the CT state is not determined. Sobolewski et al.[24] have found that, in vacuum, a $\pi\sigma^*$ state lies close to the ^1L_a state. This state is well described as having an electron removed from the ring HOMO and placed in a 2s-like orbital localized on the ring H that is bonded to the ring N. Such a state has a large dipole and might be expected to be stabilized in a polar solvent. They[25] have suggested that the variable quantum yield found for Trp in proteins might be explained by quenching through the $\pi\sigma^*$ state, given that it is antibonding in the HN bond and dissociation leads to the ground-state energy surface. This possibility seems unlikely, given the lack of quenching seen for 3MI in any solvent.

Conclusions drawn here for the variable quenching of Trp have previously been made for tyrosine.[26,27] Noronha et al.[27] reported that *N*-acetyltyrosinamide has $\Phi_f = 0.18$ in dioxane, and drops to 0.05 as the water composition of the solvent is increased to 100% at 25 °C.

Conclusion

The ad hoc model proposed by Callis, Vivian, and Liu[9,10] to explain the variation of Trp quantum yield in proteins and recently extended[14] to have physically more reasonable parameters, is upheld by this study. In this model, quenching is high when a ring to backbone amide CT state is stabilized by a locally asymmetric electrostatic environment, and has little to do with the relative electronic coupling.

Acknowledgment. This work was supported by NSF Grant MCB-0133064.

Supporting Information Available: Graphs equivalent to Figure 3 for all 36 trajectories (two chromophores in six different conformations for three solvents). This material is available free of charge via the Internet at http://pubs.acs.org.

References and Notes

(1) Eftink, M. R. *Methods Biochem. Anal.* **1991**, *35*, 127–205.
(2) Lakowicz, J. *Principles of Fluorescence Spectroscopy*, 2nd ed.; Plenum: New York, 1999.
(3) Meech, S. R.; Lee, A.; Phillips, D. *Chem. Phys.* **1983**, *80*, 317–28.
(4) Sillen, A.; Hennecke, J.; Roethlisberger, D.; Glockshuber, R.; Engelborghs, Y. *Proteins: Struct., Funct., Genet.* **1999**, *37*, 253–63.
(5) Chen, Y.; Liu, B.; Yu, H.-T.; Barkley, M. D. *J. Am. Chem. Soc.* **1996**, *118*, 9271–8.
(6) Petrich, J. W.; Chang, M. C.; McDonald, D. B.; Fleming, G. R. *J. Am. Chem. Soc.* **1983**, *105*, 3824–32.
(7) Cowgill, R. W. *Biochim. Biophys. Acta* **1970**, *200*, 18–25.
(8) Feitelson, J. *Isr. J. Chem.* **1970**, *8*, 241–52.
(9) Callis, P. R.; Vivian, J. T. *Chem. Phys. Lett.* **2003**, *369*, 409–14.
(10) Callis, P. R.; Liu, T. *J. Phys. Chem. B* **2004**, *108*, 4248–59.
(11) Chen, J. J.; Flaugh, S. L.; Callis, P. R.; King, J. *Biochemistry* **2006**, *45*, 11552–63.
(12) Xu, J. H.; Toptygin, D.; Graver, K. J.; Albertini, R. A.; Savtchenko, R. S.; Meadow, N. D.; Roseman, S.; Callis, P. R.; Brand, L.; Knutson, J. R. *J. Am. Chem. Soc.* **2006**, *128*, 1214–21.
(13) Kurz, L. C.; Fite, B.; Jean, J.; Park, J.; Erpelding, T.; Callis, P. *Biochemistry* **2005**, *44*, 1394–413.
(14) Callis, P. R.; Petrenko, A.; Muiño, P. L.; Tusell, J. R. *J. Phys. Chem. B* **2007**, *111*, 10335–9.
(15) Wasielewski, M. R.; Johnson, D. G.; Niemczyk, M. P.; Gaines, G. L.; Oneil, M. P.; Svec, W. A. *J. Am. Chem. Soc.* **1990**, *112*, 6482–8.
(16) Eftink, M. R.; Jia, Y.; Hu, D.; Ghiron, C. A. *J. Phys. Chem.* **1995**, *99*, 5713–23.
(17) Yu, H. T.; Colucci, W. J.; McLaughlin, M. L.; Barkley, M. D. *J. Am. Chem. Soc.* **1992**, *114*, 8449–54.
(18) Ridley, J.; Zerner, M. *Theor. Chim. Acta (Berlin)* **1973**, *32*, 111–34.
(19) Bixon, M.; Jortner, J. *Adv. Chem. Phys.* **1999**, *106*, 35–202.
(20) Kestner, N. R.; Logan, J.; Jortner, J. *J. Phys. Chem.* **1974**, *78*, 2148–66.
(21) Tachiya, M. *J. Phys. Chem.* **1993**, *97*, 5911–6.
(22) Hopfield, J. J. *Proc. Natl. Acad. Sci. U.S.A.* **1974**, *71*, 3640–4.
(23) Loring, R. A. *J. Phys. Chem.* **1990**, *94*, 513–5.
(24) Sobolewski, A. L.; Domcke, W.; Dedonder-Lardeux, C.; Jouvet, C. *Phys. Chem. Chem. Phys.* **2002**, *4*, 1093–100.
(25) Dedonder-Lardeux, C.; Jouvet, C.; Perun, S.; Sobolewski, A. L. *Phys. Chem. Chem. Phys.* **2003**, *5*, 5118–26.
(26) Cowgill, R. W. *Arch. Biochem. Biophys.* **1963**, *100*, 36–44.
(27) Noronha, M.; Lima, J. C.; Lamosa, P.; Santos, H.; Maycock, C.; Ventura, R.; Macanita, A. L. *J. Phys. Chem. A* **2004**, *108*, 2155–66.

JP711513B